Solution, Phase Coexistence, and Related Proton Nuclear Magnetic Resonance Studies on Poly-L- and Poly-DL-alanine in Helix–Random Coil Interconverting Media*

Akira Takahashi,† L. Mandelkern, and R. E. Glick

ABSTRACT: Various solution properties of poly-DL-alanine and poly-L-alanine in trifluoroacetic acid–chloroform media have been studied over a range of temperatures. In addition to homogeneous solutions at high acid content, both poly-DL- and poly-L-alanine display phase separation in the lower acid range. The DL-polypeptide is found to separate into two liquid phases while the L-polymer exhibits both liquid–liquid and liquid–solid regions. Phase stability and intrinsic viscosity studies on the DL-polymer result in postulating that the DL-polymer is in the random coil configuration throughout the solvent composition range examined. Proton nuclear magnetic resonance spectral data obtained under comparable conditions of solvent composition and temperature are consistent with this configurational assignment. Poly-L-alanine solution phase stability, intrinsic viscosity and proton nuclear magnetic resonance spectral characteristics differ significantly from the corresponding poly-DL-alanine solution properties. In the homogeneous region the present results augment and expand upon those previously reported in the literature. In particular, it is concluded by appropriate contrasting of solution properties that poly-L-alanine is in the random coil configuration in 100% acid, is helix–random coil interconverting in a manner characteristically found for polymers undergoing cooperative transitions in 70–100% acid, and is in a helical configuration of varying nature from 20–70% acid. At the lower end of the temperature range and between 90 and 100% acid, there is a suggestion that the L-polypeptide is more stable in the randon coil than the helical configuration. Proton nuclear magnetic resonance spectral data for poly-L-alanine in the region of liquid–liquid phase separation are consistent with an ordered or helical polypeptide in both of the phases. X-Ray evidence is presented to indicate that ordered polymer is also precipitated in the liquid–solid region. In the phase separation region and at low temperatures, nuclear magnetic resonance line widths for both poly-L- and poly-DL-alanine broaden. These parallel results are interpreted as due to aggregation rather than indicating conformational changes as has been suggested for L-polymer.

In previous reports (Glick *et al.*, 1966; Stewart *et al.*, 1967a,b) high resolution proton nmr spectra of PLA[1] and PDLA in helix–random coil interconverting media were contrasted and interpreted in terms of both polymer–solvent interactions (Stewart *et al.*, 1967b) and polymer structure (see also, Markley *et al.*, 1967). A subsequent report on PLA (Bradbury and Rattle, 1968) was concerned with further aspects of the correlation of structure and spectra affected by solvent, solution temperature, and solute molecular weight. Inasmuch as the alanine structural unit provides the basis for a spectrally simple system exhibiting helix–coil interconversion, the contrasts between PLA and PDLA can provide reference characteristics for similar systems. Toward this end, we wish to report the results of detailed studies of (1) dilute solution properties of both PLA and PDLA in the interconverting medium, trifluoroacetic acid–chloroform-*d*; (2) concentrated solution properties as reflected by polymer–solvent three component phase diagrams; and (3) proton magnetic resonance spectra complementing 1 and 2. These results provide further information relevant to the size, shape, molecular structure, and interactions of the polypeptides in their various configurations.

Methods and Materials

Two samples of PLA (I and II) and a low molecular weight sample of PDLA were obtained from Pilot Chemical Co. A high molecular weight sample of PDLA was kindly supplied by Drs. Y. Iwakura and M. Oya of the University of Tokyo. The polymers were dried *in vacuo* at 100° and stored in a phosphorus pentoxide desiccator.

* From the Department of Chemistry and Institute of Molecular Biophysics, The Florida State University, Tallahassee, Florida 32306. *Received October 22, 1968.* This work was supported in part by U. S. Public Health Service Research Grants G. M. 11337 and G. M. 10614, and in part by a contract between the Division of Biology and Medicine, U. S. Atomic Energy Commission, and The Florida State University. Part of this paper was presented before the 153rd National Meeting of the American Chemical Society, Miami Beach, Fla. 1967.

† Permanent address: Department of Applied Chemistry, Nagoya University, Nagoya, Japan.

[1] Abbreviations used: PDLA, poly-DL-alanine; PLA, poly-L-alanine; TFA, trifluoroacetic acid.

Trifluoroacetic acid and dichloroacetic acid were distilled over phosphorus pentoxide and stored in a polyethylene drybox. Spectrophotometric grade chloroform (Baker) was used without further treatment, since it was observed that when the ethanol stabilizer was removed the solution became yellow. 2,2,2,-Trifluoroethanol was obtained from Matheson Coleman and Bell, $CDCl_3$ from Merck Sharp and Dome (Canada), and tetramethylsilane from Stauffer; all were used without further treatment.

Weight-average molecular weights for the samples of PLA were determined at 25° by light scattering as measured in a SOFICA photometer with an incident wavelength of 5461 Å. The solvent selected was dichloroacetic acid. It was necessary to heat the dichloroacetic acid solution for 1 hr at 100° to ensure dissolution. After cooling the solution, measurements of both light scattering and refractive index increment were carried out immediately. The value of dn/dc, measured with a Brice-Phoenix differential refractometer, was 0.070 cc/g at 5461 Å. Solvent and solutions were filtered through VF-6 and α-8 membranes (Gelman) and an α-8 membrane sandwiched between two VF-6 membranes. The error in these determinations was estimated to be 20%.

Number-average molecular weights for the samples of PDLA were determined by osmometry at 30°. 2,2,2-Trifluoroethanol was found to be a suitable solvent. The Mechrolab high-speed membrane osmometer, Model 502, fitted with gel cellophane 600 and conditioned by the standard method was used in these determinations. Although the molecular weight of one sample was very low, *ca.* 3000, there was no indication of any solute permeation through the membrane.

Intrinsic viscosities of both PLA and PDLA, in various mixtures of TFA and $CHCl_3$, were measured with a Cannon-Ubbelohde viscometer at 25 ± 0.05°. Since the polymer might be degraded by TFA, all measurements were completed within 2 hr after a solution was prepared.

Two methods were used to determine phase-separation binodials for the ternary system polypeptide–TFA–$CHCl_3$. The first, a titration method, was carried out in a thermostated, magnetically stirred cell fitted with 10-ml burets that served to introduce the pure solvents, TFA and $CHCl_3$. To avoid hydration, drying tubes were attached to the burets. A predetermined weight of polymer was dissolved in the cell by adding TFA. The solution was titrated with $CHCl_3$ until blurring or turbidity appeared. Further addition of TFA was followed by $CHCl_3$ titration. This process was repeated so that binodials for decreasing polymer concentration were produced.

In the second method, the polymer was placed in a test-tube-shaped cell with a buret attached to the top of the cell and with a small condenser at the side. After the addition of a specific mixture of TFA–$CHCl_3$, the polymer could be dissolved by gradually increasing the temperature. Upon sample dissolution, the temperature was lowered, at a speed of 10°/20 min, and the temperature, T_p, at which turbidity occurred was determined. A dissolution temperature, T_d, was obtained by raising the temperature of the turbid solution.

Tie lines were determined by direct analysis of the appropriate phases. The polymer was placed in a graduated centrifuge tube fitted with a ground-glass stopper. After addition of a specific mixture of TFA–$CHCl_3$, the polymer could be dissolved by gradually increasing the temperature. Upon sample dissolution, the temperature was gradually lowered, brought to a specified temperature, and allowed to stand overnight; two clear liquid phases appeared.

The upper phase was the concentrated polymer phase. After recording the volume of each phase, the lower phase was separated with a syringe fitted with a Teflon needle, the solution was injected into standardized NaOH and the acid concentration was determined by back-titration with standardized HCl solution using phenolphthalein as an indicator. The upper phase was washed into a weighing bottle, vacuum dried in a KOH desiccator, and finally dried at 100° in a vacuum oven for 3 days. The residue provided the polymer concentration in the upper phase. The specific volume of polypeptide was assumed to be 0.78 cc/g (Flory and Leonard, 1965).

In the liquid-crystal-phase separation region of PLA–TFA–$CHCl_3$, the upper phase consisted of a powdery solid. The solid was transferred into a Petri dish and dried under vacuum over KOH for 3 days at room temperature. Powdered specimens were sealed in 0.3-mm glass capillaries, Unimex-Caine Corp., which were then positioned in a Norelco generator set at 40 kV and 20 mA. The exposure time was 24 hr. The *d* spacings were calculated from the diametrical spacings on the film.

Nmr spectra were obtained on a Varian HA-60 high-resolution nmr spectrometer with Model V-4311 RF unit and variable temperature probe that allowed for thermal precision within 1°. Chemical shifts were read as recorded against tetramethylsilane as an internal standard. Line widths and areas were measured at a radiofrequency magnetic field below saturation. Areas were integrated by a planimeter and were compared to that due to the small amount of nondeuterated chloroform in the solvent. The error in this determination was estimated to be no greater than 10%. Special care attended the analysis of solutions that were phase separated to ensure that the appropriate phase was within the sample coil.

Results

Molecular Weights. Table I provides the results of the molecular weight determinations. Both PLA samples are seen to have reasonably similar molecular weights, while the PDLA samples differed markedly.

Intrinsic Viscosities. The variation of intrinsic viscosities for PLA and PDLA with solvent composition is given in Figure 1. It may be noted in Figure 1 that a sharp minimum occurs in $[\eta]$ at *ca.* 83% TFA for PLA. This transition point coincides with the midpoint in the transition region both for $-b_0$ and proton chemical shifts previously reported (Stewart *et al.*, 1967a,b). In the

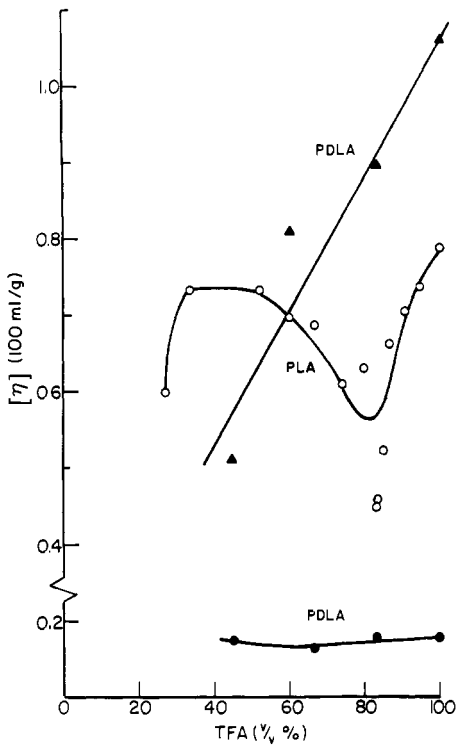

FIGURE 1: Variations of intrinsic viscosities *vs.* mixed-solvent composition at 25°. (○) Poly-L-alanine I, (▲) poly-DL-alanine II, and (●) poly-DL-alanine I.

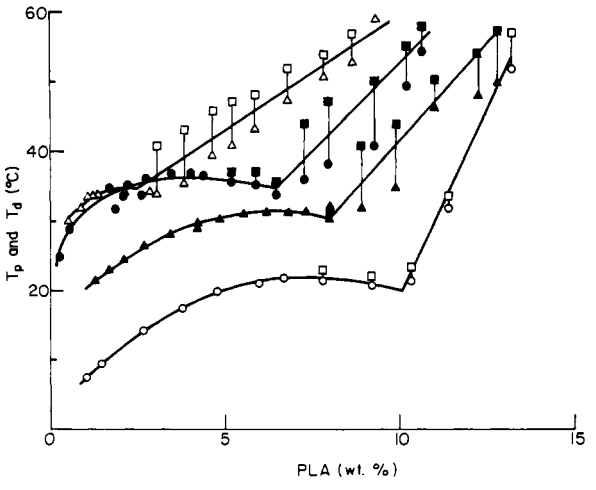

FIGURE 2: Phase-separation temperature, T_p, and dissolution temperature, T_d, *vs.* poly-L-alanine concentration. (Poly-L-alanine II) trifluoroacetic acid (%): △ and △—□, 15; ○ and ●—■, 20; ▲ and ■—▲, 30; and ○ and □—○, 40. The symbol such as □—○ indicates that □ ≡ T_d and ○ ≡ T_p.

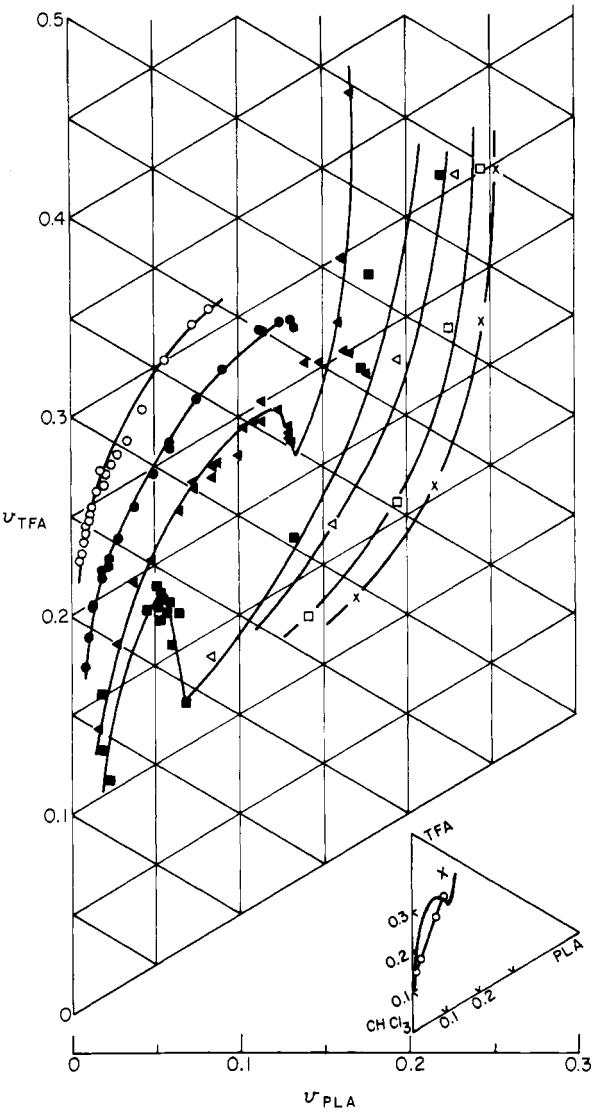

FIGURE 3: Phase diagrams of the system poly-L-alanine–trifluoroacetic acid–chloroform-*d* at various temperatures. Temperature (°C): ○, 25; ●, 29; ▲, 32; ■, 34; △, 40; □, 50; and X, 55. Inserted triangular-phase diagram shows the binoidial and tie lines at 25.

TABLE I: Molecular Weight of Poly-L- and -DL-alanine.

Sample	Mol Wt (g)	DP
Poly-L-alanine I	37,000 ± 8,000	500
Poly-L-alanine II	33,000 ± 7,000	450
Poly-DL-alanine I	2,900 ± 100	40
Poly-DL-alanine II[a]	24,000 ± 1,000	340

[a] Supplied by Drs. Iwakura and Oya. Prepared from *N*-carboxy-DL-alanine anhydride polymerized in acetonitrile (Oya *et al.*, 1966).

region between 30 and 50% TFA, [η] of PLA decreases slightly; below 25% TFA, data obtained by the method employed are unreliable since phase separation occurs. As contrasted in Figure 1, [η] for PDLA decreases monotonically as TFA decreases. The variation is larger for the higher molecular weight PDLA than for the lower molecular weight sample; for the latter, the change is very small. Determination of [η] on PDLA could not be extended to low acid solutions because such solutions become turbid at room temperature in the range 35–40% TFA.

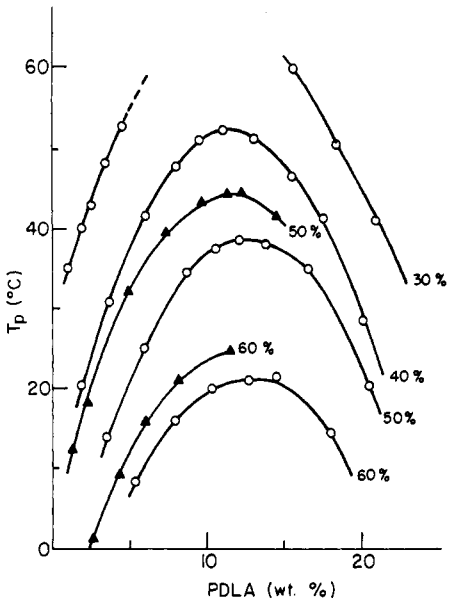

FIGURE 4: Phase-separation temperature *vs.* poly-DL-alanine concentration. Trifluoroacetic acid per cent are indicated; (○) poly-DL-alanine I and (▲) poly-DL-alanine II.

Phase Diagrams. A. *System PLA–TFA–$CHCl_3$.* Phase diagrams at different temperatures for the system of PLA–TFA–$CHCl_3$ (PLA II was used) are shown in Figures 2 and 3. In Figure 2, the phase-separation temperature, T_p, and dissolution temperature, T_d, are plotted against the polymer concentration at each of the specified compositions of the mixed solvents. There are two distinct intersecting regions. In the left convex curve region, T_d and T_p coincided within 0.5°; the occurrence of turbidity and its disappearance are completely reversible so that no perceptible supercooling is observed. Below the convex curve region, liquid–liquid phase separation occurs. Both phases are transparent; the upper phase is more viscous than the lower phase. Examination of both phases under the polarizing microscope revealed no birefringence.

In the right region, there were fairly large differences between T_d and T_p with $T_d > T_p$. In this region, after phase separation at 25°, the lower phase was transparent while the upper phase contained a powdery solid.

Triangular phase diagrams at different temperatures are shown in Figure 3. The correspondence between two figures, Figures 2 and 3, is obvious. The left convex region coincides with the liquid–liquid-phase separation region, while the right region indicates liquid–solid-phase separation. The insert in Figure 3 provides the tie lines and binodials at 25°.

B. *System PDLA–TFA–$CHCl_3$.* Phase diagrams for both PDLA samples are shown in Figures 4 and 5. As is indicated, all curves are convex. Curves for the higher molecular weight samples appear above the corresponding curve for the lower molecular weight material. The monotonically increasing curve of Figure 2 is absent in the case of PDLA. In the triangular phase diagram of Figure 5, tie lines are also indicated. The open circles are plait points, their extrapolation to infinite molecular weight determines the critical consolute mixture which corresponds to the θ point for random-coiled polymers (Flory, 1953). Since only two samples of different molecular weight were used, great accuracy in the determination of the critical consolute mixture would not be expected. The critical consolute mixture at 25° is located at 45% TFA.

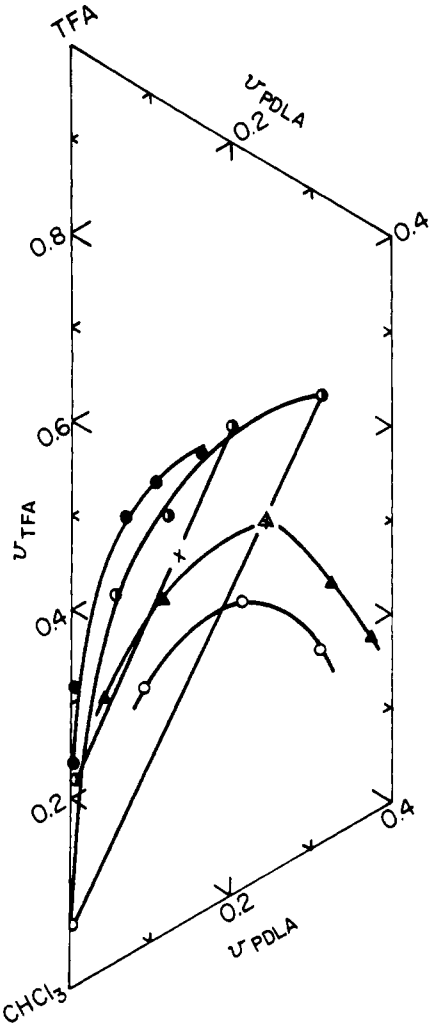

FIGURE 5: Phase diagrams of poly-DL-alanine–trifluoroacetic acid–chloroform-*d* systems. (●) Poly-DL-alanine II at 25°, (◑) poly-DL-alanine) I at 25°, (△) poly-DL-alanine I at °, and (○) poly-DL-alanine I at 40°. X indicates original composition of the system.

X-Ray Powder Pattern. The observed *d* spacings (in ångströms) are shown in Table II, together with *d* spacings for both the α-helical and the extended β form of PLA. The powder pattern indicates the presence of both forms. We have not attempted a quantitative analysis. It may only be inferred that the solid examined is that in equilibrium with liquid phase.

Proton NMR Studies; Spectra and Spectral Temperature Variations. The proton magnetic resonance spectrum of a dilute solution of PLA in TFA, as previously reported (Glick *et al.*, 1966; Stewart *et al.*, 1967a,b; Markley *et al.*, 1967; Bradbury and Rattle, 1968),

TABLE II: Comparison of Spacings (in Ångströms) α, β, and precipitated Poly-L-alanine

Spacings for Form		Precipitated from	
α-Poly-L-alanine[a]	β-Poly-L-alanine[b]	6.3% Poly-L-alanine 18.7% Trifluoroacetic Acid	8.3% Poly-L-alanine 27.0% Trifluoroacetic Acid
7.40 (s)		7.47 (vs)	7.50 (vs)
		5.71 (m)	5.70 (m)
		5.11 (m)	5.08 (m)
	4.37 (s)	4.38 (s)	4.35 (s)
4.28 (m)			
	4.26 (mw)		
3.70 (m)	3.73 (m)	3.73 (s)	3.72 (s)
	2.98 (m)		
1.495 (vw)		1.509[c]	1.507[c]
		1.431 (mw)	1.482
	1.147 (m)	1.159	1.155

[a] Brown and Trotter (1956). [b] Bamford *et al.* (1956). [c] Two closely spaced reflections.

consists of three main polypeptide absorption peaks arising from the amide proton, the methyne proton, and the side-chain methyl protons. The methyl absorption (CH_3) appears as a nearly symmetric doublet with the peak separation of 6.0 (0°) to 6.8 Hz (at 55°) and a half-width of about 14 Hz; the methyne absorption (CH) is split into a broad, reasonably symmetric triplet with component separations of about 6.5 Hz and half-width of about 18 Hz, while amide proton (NH) absorption is split into a narrow almost symmetric doublet with component separation of about 6 Hz and line width of about 13 Hz. Spin–spin interactions were confirmed by homonuclear decoupling. The spectral details reported here are identical with those of Markley *et al.* (1967). However, Bradbury and Rattle (1968) present spectra without NH and CH splittings. Spectral changes accompanying variations in TFA–$CDCl_3$ ratio at several temperatures are shown in Figures 6–8 for PLA.

The right-hand side represents the homogeneous region in these figures. As is indicated in Figure 6, the position of PLA–CH varies monotonically as the TFA concentration is increased until about 70–80% acid where a change in slope is noted. (See also Markley *et al.*, 1967). Changes in temperature resulted in parallel effects with the signal moving upfield with increasing temperature. The signal for PLA–CH_3 varies in a somewhat more complicated manner. At 0° the chemical shift is displaced slightly downfield as the acid concentration is reduced. Above 5°, however, the downfield displacement reaches a limit at about 57% acid and then the peak moves upfield as the TFA concentration decreases. In general the CH_3 signal is an almost symmetric doublet, becoming a singlet both at temperatures less than 10° and for acid concentrations below 80%. The NH chemical shift of PLA generally remains constant or moves upfield as the temperature is changed from 0 to 55°. Above 25°, NH moves upfield in the TFA range 18–25%, remains constant through the region 25–70%, and then moves upfield again from 70 to 100% acid. At 0 and 15°, on the other hand, NH is constant to 80% acid, moves upfield to 90% then, as an exception, downfield in pure TFA.

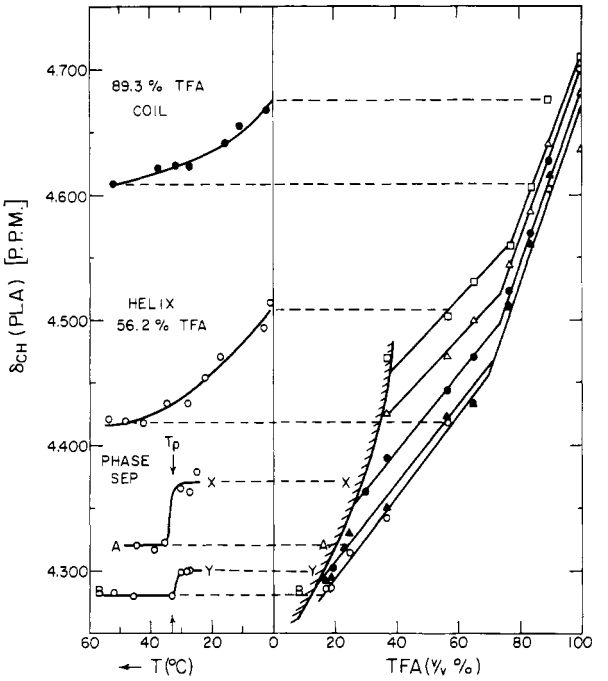

FIGURE 6: α-CH proton chemical shift (δ_{CH}) of poly-L-alanine *vs.* trifluoroacetic acid composition and temperature. Temperature (°C) ■ (in the right-hand-side figure) □, 0; △, 15; ●, 7 plus 40; and ○, 50. Left-hand side-figure: (●) trifluoroacetic acid per cent = 89.3, (○) trifluoroacetic acid per cent = 56.2, and (○) phase-separation system.

Nmr data for PDLA are shown in Figure 9. Here, PDLA–NH moves linearly upfield both with decreasing acid and increasing temperature. The PDLA–CH signal is displaced linearly throughout the entire acid range examined and in a parallel manner as the temperature is varied. PDLA–NH and –CH are broad singlets.

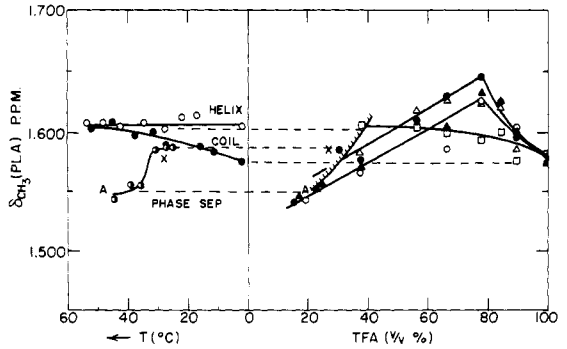

FIGURE 7: CH_3 proton chemical shift (δ_{CH_3}) of poly-L-alanine *vs.* trifluoroacetic acid composition and temperature. Symbols for both left- and right-hand side figures are the same as in Figure 6.

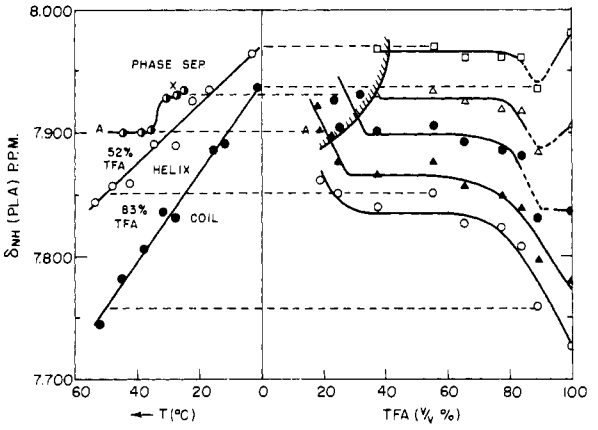

FIGURE 8: NH proton chemical shift (δ_{NH}) of poly-L-alanine *vs.* trifluoroacetic acid composition and temperature. Symbols for figures are the same as in Figure 6.

PDLA–CH_3 is a doublet in 100% acid. The separations are as in PLA–CH_3. The doublet collapses to a singlet at low temperature, 3°, and at all temperatures in 38.8% TFA. Displacements of PDLA–CH_3 varied linearly with both acid concentration and temperature.

No specific spectral changes accompanied variations in concentration of either polypeptide, except those to be described below in the region of phase separation. In Figures 6–9, the shaded zone indicates the phase separation region.

NMR Peak Area and Line Width. In the single-phase region, the ratio of peak area of CH, NH, and CH_3 is found to be 1:1:3. In the phase separation region, separate polypeptide signals are found in each phase (Figure 10 and see below). The separate phase area ratios for each resonance reflect the concentration of polypeptide in each phase as can be anticipated from the tie-line determinations. The various experimental quantities for PLA II are given in Table III, and in Figure 10 for two different initial conditions. The spectral areas for each proton of PLA at phase separation are shown. The temperature at which the peak area changes occurred coincides with the phase separation temperature.

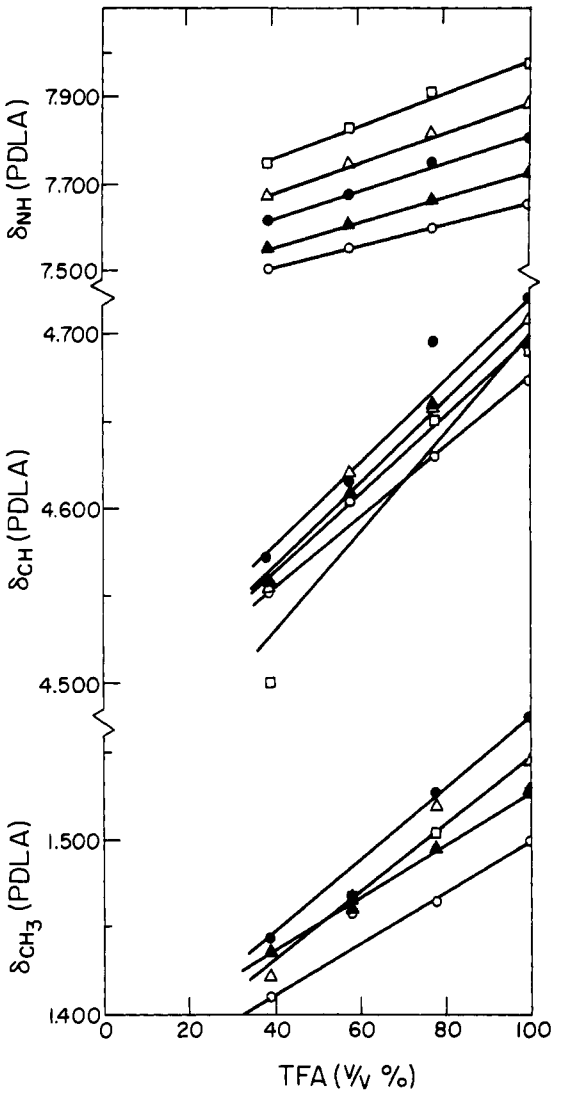

FIGURE 9: Chemical shift of NH, α-CH, and CH_3 of poly-DL-alanine *vs.* trifluoroacetic acid composition at different temperatures. □, 0°; △, 15°; ●, 27 + 40° and ○, 50°.

Figure 11 displays the variations of nmr line width with temperature and solvent composition. Above the phase-separation temperature the line widths of PLA protons are almost unchanged. Below T_p the line widths broaden, with the broadening for NH > CH > CH_3. The temperature at which broadening occurred coincides with the phase separation temperature.

Line widths of PDLA peaks, which are not illustrated, are almost independent of both temperature and acid composition except near conditions for phase separation. PDLA–NH varies with temperature (3–47.5°) in the range 15–16 Hz, 100% TFA, to the range 17–19 Hz, 58% TFA. In 38.8% TFA, a point near phase separation, PDLA–NH increases from 21 to 28 Hz in the temperature range 47.5–3°. PDLA–CH line widths at points corresponding to NH observations are about 20 Hz at 58% TFA and above and vary from 20 to 29 Hz in the 38.8% TFA temperature range cited above. PDLA–CH_3 singlet formation is also

TABLE III: Comparison of the Results of Poly-L-alanine Concentration Determination in Each Phase by Nuclear Magnetic Resonance and from Phase Diagrams.

	System A	System B
Original poly-L-alanine volume Fraction ($v_{0\,\text{Poly-L-alanine}}$)	0.065	0.029
Original trifluoroacetic acid volume Fraction ($v_{0\,\text{Trifluoroacetic Acid}}$)	0.23	0.19

	Phase Diagram	Peak Area
$v_{\text{Poly-L-alanine}}$ (concentrated phase)/ $v_{0\,\text{Poly-L-alanine}}$ (original)	1.46	1.64 (CH) 1.33 (NH) 1.66 (CH_3)

	Phase Diagram	Peak Area
$v_{0\,\text{Poly-L-alanine}}$ (original)/ $v_{\text{Poly-L-alanine}}$ (dilute phase)	3.60	3.60 (CH) 3.60 (NH) 3.61 (CH_3)

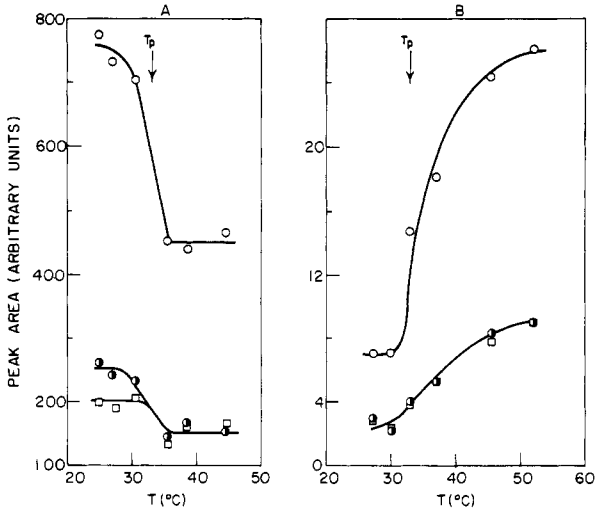

FIGURE 10: Variation of area under each peak of poly-L-alanine *vs.* temperature for phase separating system. (○) CH_3, (◑) CH, and (□) NH.

observed at the lowest, 38.8%, TFA concentration. Comparable broadening is observed near phase separation as was the case for PLA.

Discussion

Configuration of Poly-DL-alanine in the Solvent System Trifluoroacetic Acid–Chloroform. In order to interpret the nmr spectra and to contrast the PDLA and PLA data it is necessary to specify the polypeptide conformation in the various situations, *i.e.*, in both the homogeneous and heterogeneous region. Very strong evidence exists for assigning the random coil configuration to PDLA in TFA–$CHCl_3$ mixtures in all situations. In the homogeneous regions, as is indicated in Figure 1, the intrinsic viscosity decreases as the acid content decreases. This result is to be expected from general polymer solution theory for random

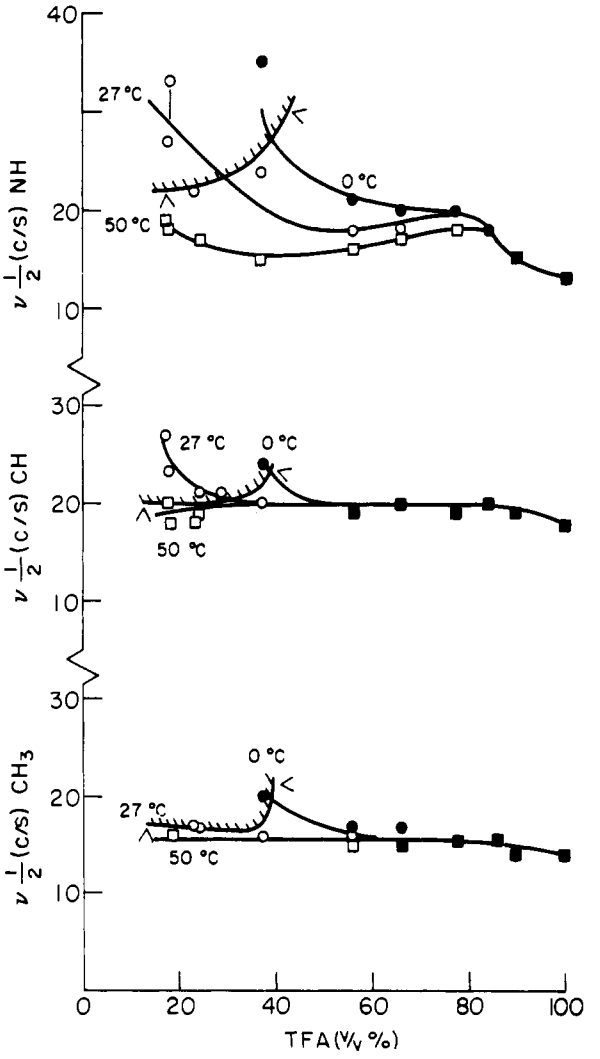

FIGURE 11: Variation of line width of each proton of poly-L-alanine *vs.* solvent composition. Temperature (°C): ●, 0; ○, 27; and □, 50.

coils (Flory, 1953) as the coil size is reduced due to a decrease in polymer–solvent interaction. In addition, analysis of the liquid–liquid binary-phase diagram provides the critical consolate mixture at 25°. Under these conditions a randomly coiled polymer solution behaves as though it were ideal (Flory, 1953) and the intrinsic viscosity should be proportional to the square root of the molecular weight. In work to be reported in detail elsewhere (A. Takahashi, L. Mandelkern, and R. E. Glick, to be published), we have found that under the aforementioned conditions, $[\eta]$ for PDLA is proportional to $M^{1/2}$. The characteristic ratio for chain dimensions that are deduced are compatible with theoretical calculations (Miller *et al.*, 1967).

The liquid–liquid-phase separation observed is most commonly associated with random coil polymers. However, as will be discussed below, the observation of this phenomena is not necessarily unique to the random coil configuration. We do note that for PDLA, as contrasted with PLA, liquid–solid-phase separation with the precipitation of an ordered phase is absent.

Finally, we observe in Figure 9 that proton nmr chemical shifts for PDLA are linear functions of solvent composition and temperature. This indicates a constant configuration throughout the region of this investigation and is consistent with the random coil configuration assignment for PDLA in TFA–$CHCl_3$ mixtures.

Configuration of Poly-L-alanine in Homogeneous Mixtures of PLA–TFA–$CHCl_3$. In dilute solutions of PLA, at solvent compositions where one homogeneous phase is maintained, there is abundant evidence that a helix–coil transition occurs at room temperature when the TFA concentration exceeds 70% by volume. As has previously been reported (Stewart *et al.*, 1967a,b; Bradbury and Rattle, 1968), changes in the proton nmr frequencies as a function of acid concentration correlate very well with the change in optical rotatory dispersion under the same conditions. Although it was postulated that the latter observations did not necessarily require a helix–coil transition, the present intrinsic viscosity results add further strong substantiation to the occurrence of such a transition.

PLA Intrinsic Viscosity, Single Phase. The change in $[\eta]$ of PLA with solvent composition, Figure 1, is best discussed by dividing the results into four regions: (a) in the high acid region, $[\eta]$ parallels that of PDLA; (b) in the region 50 to 85% TFA, $[\eta]$ shows a sharp minimum; (c) in the region 30 to 50% TFA, $[\eta]$ is constant, and (d) in very low acid, 30% TFA, $[\eta]$ decreases again. The solvent induced variation of $[\eta]$ for PLA can be interpreted in terms of the basic theory for polymer intrinsic viscosity for randomly coiled (Flory and Fox, 1951) and broken rod or wormlike macromolecules (Eizner and Ptitsyn, 1962; Yu and Stockmayer, 1967; Nagai, 1961). The decrease in $[\eta]$ for PLA in the high acid region parallels that for PDLA as would be expected for a random-coiled polymer for the reasons cited above. The large increase in $[\eta]$ as the acid concentration is decreased from 85 to 50% is attributed to a change in the polymer chain conformation; the increased $[\eta]$ being consistent with the formation of a more extended structure. The constancy of $[\eta]$ in the region of 30–50% TFA is consistent with an extended ordered structure with minimal changes in dimensions induced by solvent interactions. The slight decrease in $[\eta]$ in the very low acid region could be due to aggregation effects, since the composition involved is that where incipient phase separation would be expected.

The intrinsic viscosity variations indicate that a cooperative conformational change occurs at about 80% acid. The data cited previously identifies this with a helix–coil transition. Recent calculations of the unperturbed end-to-end distance for polypeptides as a function of helical content showed that a minimum should occur in $[\eta]$ for a certain range of molecular weights (Nagai, 1961; Flory and Miller, 1966). The intrinsic viscosity results reported here for PLA support these calculations. It was also observed that plots of the reduced viscosities, *i.e.*, η_{sp}/c against polymer concentration, c, were linear functions of c for mixtures of TFA–$CHCl_3$. This indicates the absence of important polyelectrolyte effects,[2] *i.e.*, acid proton transfer to the polypeptide.

PLA and PDLA Proton NMR Features, Single Phase. The feature of the proton nmr spectra of PLA and PDLA most amenable to elaboration is the solvent induced variation of the CH resonance (Stewart *et al.*, 1967a,b; Markley *et al.*, 1967; Bradbury *et al.*, 1967). The methyl proton spectral variations are small (Figures 7 and 9). The changes in the amide proton (Figures 8 and 9) are complicated by exchange, and particular nmr relaxation effects (Stewart *et al.*, 1967a). Various configurational changes and interactions appear therefore to be adequately described by differences in PDLA- and PLA–CH resonance frequencies, $\Delta\delta_{CH}$.

In Figure 12, $\Delta\delta_{CH}$ are plotted as a function of temperature for specified TFA concentrations. In Figure 13, $\Delta\delta_{CH}$ are plotted as a function of solvent composition at four different temperatures 0, 15, 27, and 50°. These difference frequencies are seen to be greatest both at high temperature and low acid, corresponding at these extremes to a helical configuration for PLA as contrasted to the random coil configuration for PDLA. This difference can be interpreted by considering that, in the helix, the position of the various groups are held fixed. Hence, anisotropic shielding effects associated with the carbonyl bond, and to a lesser extent other bonds, may make a fairly large contribution to shielding for atoms held near the bond axis. In the random coil conformation of the polypeptide, motion of the

[2] Hanlon and Klotz have suggested from infrared and conductance measurements (Hanlon and Klotz, 1965; Stake and Klotz, 1966; Hanlon, 1966) that polypeptides are protonated at the amide moiety by trifluoroacetic acid in trifluoroacetic acid–chloroform-*d* mixture. They thereby concluded that the change in $-b_0$ does not reflect helical destruction. Our own studies, both nuclear magnetic resonance and hydrodynamic evidence which parallels the $-b_0$ change, rule out their suggestion. The same conclusion has been reached on similar systems by Quadrifoglio and Urry (1967) from circular dichroism studies and by Bradbury and Rattle (1968) from infrared studies.

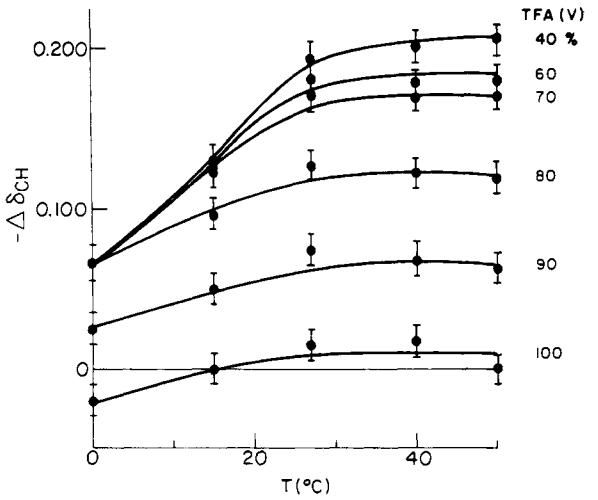

FIGURE 12: Difference CH chemical shifts of poly-DL-alanine and poly-L-alanine in trifluoroacetic acid–$CDCl_3$, $(\delta_{CH})_{PDLA} - (\delta_{CH})_{PLA} = \Delta\delta_{CH}$ *vs.* temperature at various trifluoroacetic acid compositions.

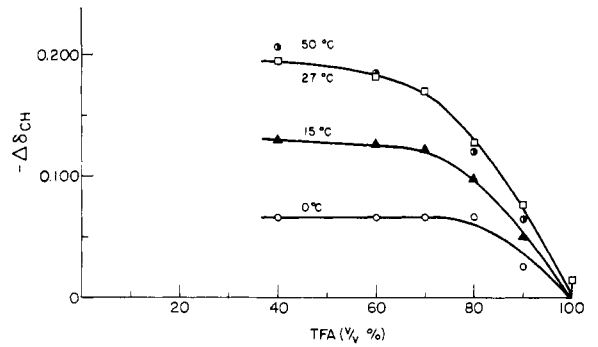

FIGURE 13: Difference CH chemical shifts of poly-DL-alanine and poly-L-alanine in trifluoroacetic acid–$CDCl_3$, $(\delta_{CH})_{PDLA} - (\delta_{CH})_{PLA} = \Delta\delta_{CH}$ *vs.* trifluoroacetic acid composition at various temperatures. Temperature (°): ◑, 50; □, 27; ▲, 15; and ○, 0.

various groups with respect to each other can occur more freely, resulting in a smoothed shielding with smaller anisotropic contributions due to neighboring features. In the α helix of PLA, CH proton is *cis* to the carbonyl and is undoubtedly affected by the carbonyl electron distribution.

Contributions to $\Delta\delta_{CH}$ due to polypeptide–TFA interaction must also be considered (Stewart *et al.*, 1967a; Bradbury and Rattle, 1968). In the discussion above, PLA is considered to be in the helical configuration when the TFA concentration is below 70%. Contrasting $\Delta\delta_{CH}$ at 0° and TFA < 70%, with $\Delta\delta_{CH}$ at higher temperature and TFA < 70%, Figure 13, suggests that solvent contributions provide a decreasing shielding contribution, *i.e.*, we assume that the temperature independence of $\Delta\delta_{CH}$ at high temperature and low acid indicates a minimum of solvent–solute interaction. Thus, $\Delta\delta_{CH}$ reflects: (1) the helix–coil transition begins at 80–85% TFA irrespective of temperature; (2) at low temperature and at TFA concentrations above 90% the polymer is completely transformed into the random coil configuration; (3) at high temperature, above 30°, and for acid concentrations between 40 and 70%, neither PLA nor PDLA appear to be interacting with solvent. Therefore, PLA should be at a helical maximum if the helix is that configuration requiring a minimum of solvent interaction; and (4) in a solvent mixture containing less than 80% TFA and at low temperature, PLA is either partially helical or interacting more effectively with solvent. This high-temperature minimum in polymer solvent interaction results in an apparent temperature stability inversion, *i.e.*, the polymer is more stable in the helical configuration at high temperature (see also Bradbury and Rattle, 1968). The same inverted helix–coil transition character has been observed for poly-γ-benzyl-L-glutamate in dichloroacetic acid–ethylene dichloride mixtures (Doty and Yang, 1956; Teramoto *et al.*, 1967; Bradbury *et al.*, 1968) and a similar behavior would be anticipated for the system under study.

This temperature-induced transition appears to occur over a limited solvent composition range. This is consistent with a mechanism for helix–coil interconversion involving the competition between intermolecular solvent–polymer interaction and intramolecular interactions within the polymer. The solvent–polymer interaction (eq 1) becomes of greater importance at high acid concentration rendering stability to the coil.

$$\text{helix} \cdots\cdots \text{trifluoroacetic acid} \rightleftharpoons \text{coil} \cdots\cdots \text{trifluoroacetic acid} \quad (1)$$

The solvent, although interacting with both forms, contributes more to the right equilibrium than the left. On either side this interaction, without proton transfer, decreases with increasing temperature.

PLA and PDLA NMR Line Widths; Peak Shape, Single Phase. In the single phase region, CH and CH_3 line widths broaden only slightly from pure TFA to 80% TFA, remain essentially constant with decreasing acid, then broaden as the acid concentration is reduced further (Figure 11). Thus the line width variations of CH and CH_3 change little as a function of configuration and temperature; broadening occurs only near and through the two-phase region and thus would appear to indicate a degree of polymer intermolecular aggregation as was also reflected in the drop in intrinsic viscosity.

On the other hand, the NH line width exhibited marked temperature dependence, the lower the temperature, the broader the signal. The NH line-width variation is fairly complicated showing a maximum at 80% TFA for each temperature in the single phase region (Figure 11) corresponding to the helix–coil interconverting region. Of further note is that NH peak is relatively narrow indicating that the nitrogen nucleus and the proton are effectively decoupled, *i.e.*, the quadrapolar broadening of the nmr absorption of a proton directly attached to an ^{14}N nucleus is not observed. As previously described for the interconversion region (Stewart *et al.*, 1967a,b) fluctuation between

coiled and helical form occur rapidly with appropriate relaxation times which are shorter than in either the helical or random coil regions. This shortening would result in the peak width variation noted.

It is also observed that the CH triplet found in 100% TFA and at low temperatures in high acid regions coalesces into a featureless peak around 80% TFA or in low acid without appreciable broadening in either case. This coalescence of the multiplet in the region of maximum helix–random coil interconversion would be expected when rapid averaging of two peak positions, helix and coil, occurs. In the low acid region, contributions from intermolecular aggregation could result in loss of peak definition.

As indicated above, both PDLA and PLA line widths broaden markedly only near the phase-separation region. As this is true for both polymers, the broadening may be attributed to intermolecular polymer interaction. This contrasts with the suggestion of Bradbury and Rattle (1968) that this is due to particular effects associated with polymer configuration, *i.e.*, as indicating restricted motion for helical PLA.

Configuration of Poly-L-alanine, Phase-Separation Region. The phase diagrams for PLA–TFA–$CHCl_3$ indicate both liquid–liquid and liquid–crystal-phase separation regions at TFA concentrations of 40% and less. This section discusses the results of the configurational studies. The fact that the proton peaks of PLA were observed even in the phase separation region indicates that the condition for motional narrowing is satisfied (Abragam, 1961). The condition is $\tau_c \ll 10^{-4}$ sec; that is, if the period of rotation of polypeptide as a whole or of the individual monomeric units is short compared to 10^{-4} sec, there will be a high resolution spectrum, and typical liquid-like line widths will be observed. If the time of rotation is comparable to 10^{-4} sec, intermediate line widths will be observed.

Configuration of PLA in Liquid–Liquid-Phase Separation Region. The determination of the configuration of PLA in the region of liquid–liquid-phase separation is based on proton magnetic resonance features given in the left-hand sides of Figures 6–8. In these figures, frequency variations for each PLA proton at three fixed acid concentrations correspond to regions where (1) the coil configuration predominates, (2) the polymer is mainly helical, and (3) phase separation is observed.

In the homogeneous regions 1 and 2, the temperature dependence of the chemical shift for CH and CH_3 is linear, irrespective of the PLA conformation. This is demonstrated by a replot of the data on the right-hand side of the figure as is indicated by the dashed lines. In the liquid–liquid-phase separation region, however, the experimentally observed variations as a function of temperature are sigmoidal, as is indicated by the open circles. The midpoints of these curves coincide with the phase-separation temperature. The change in chemical shifts in this case can be shown to be merely a reflection of the sudden change in solvent composition which accompanies the transformation from one to two liquid phases. This is demonstrated by the dashed lines in the lower portion of the figure which indicate the expected chemical shift for the appropriate temperature and solvent composition. The latter quantities are specified from the phase diagram studies previously cited. Thus the chemical shifts at phase separation are quantitatively shown to be those expected for helical PLA in a solvent whose composition is that of the appropriate phase-separated liquid. In addition, as a consequence of the absence of chemical shifts for PLA protons as a function of PLA concentration, it is shown in Figure 10 and Table III that the peak areas in the separated phases correspond quantitatively to the polymer concentration in each of the phases. It must be concluded, therefore, that PLA remains helical in both liquid phases. This is a unique and special result since usually liquid–liquid-phase separation involves the random coil conformation of a long-chain molecule (Flory, 1953).

Configuration of PLA in Liquid–Solid-Phase Separation Region. Wide-angle X-ray patterns of these specimens demonstrate unequivocally that an ordered phase is precipitated. A comparison, in Table II, between the d spacings attributed to the α-helix and the β form with that actually observed indicates that a mixture of both ordered structures is developed under conditions of precipitation. The fact that T_d is much greater than T_p is also characteristic of a three-dimensional ordering or crystallization process where a nucleation act is rate controlling (Mandelkern, 1964). The liquid phase, prior to precipitation in the relatively low acid concentration region, contains polypeptide whose nmr spectra is characteristic of the helical form. That the PLA phase is helical is in accord with theoretical predictions that the ordered phase remains ordered with increasing polymer concentration (Flory, 1956).

Conclusion

Physical property and proton nmr studies of TFA–$CHCl_3$–PDLA and TFA–$CHCl_3$–PLA solutions have been shown to provide data relevant to polymer configurations and interactions. In the former case data for PDLA solutions have been interpreted as indicating that PDLA possesses the random coil configuration throughout the range of TFA–$CHCl_3$ examined. This range includes concentrations below 40% acid where liquid–liquid-phase separation occurs.

By contrasting PLA solution and nmr data with that for PDLA, various PLA configurations have been deduced. It is shown, as in Figure 12 and 13 for example, that PLA–PDLA difference CH shifts vary characteristically with temperature and solvent composition. In 100% TFA, $\Delta\delta_{CH}$ is temperature independent and approximately zero; in 70–40% TFA, $\Delta\delta_{CH}$ is a minimum but non-zero, at 0°, rises to a maximum value near 30° and remains constant to 50°. Intermediate behavior in $\Delta\delta_{CH}$ is observed for 90 and 80% TFA solutions in the indicated temperature range. These results have been interpreted, at all temperatures examined as indicating that in 100% TFA, PLA is a random coil; in the range from 100 to 70%, PLA is in the interconverting helix into random coil region; and below 70% TFA, PLA is helical. It has been also demonstrated that ordered PLA is observed

in TFA–$CHCl_3$–PLA solutions that phase separate into either liquid–liquid or liquid–solid PLA-containing phases.

Although PLA solvent induced chemical shifts at room temperature have been previously correlated with corresponding variations in the Moffitt rotatory parameter, b_0, and thereby reenforcing polymer configuration assignments based on this parameter, it was concluded previously that neither measured the degree of helicity of PLA in TFA–$CHCl_3$ mixtures (Stewart *et al.*, 1967a). This contention can be further supported by additional consideration of the solvent and temperature dependence of PLA–CH chemical shifts.

Nmr CH chemical shift data at various temperatures and TFA concentrations have been given for PLA in Figure 6. It may be noticed that δ_{CH} is large. At 50° as an extreme, δ_{CH} varies by 0.4 ppm in the range 100–20% TFA. A measure of the temperature variation of δ_{CH} at about 90% TFA, is reflected in the upper left-hand portion of Figure 6 for the coil and for the helix, about 56% TFA, in the center left-hand portion. It is clear that if the polymer were in a final state in 56% TFA, *i.e.*, 100% helical and without direct solvent–polymer interaction, temperature- or solvent-dependent effects in δ_{CH} of the magnitude found would not be expected. Assuming that the general aspects of the configurational assignment are correct, δ_{CH}(PLA) must reflect either (1) a change in helical content of the polymer or intrahelix dimensions, and/or (2) changes in polymer–solvent interactions.

Helical content or dimensional variations should result in a corresponding change in b_0; but b_0 is found not to vary either as a function of acid concentration, 70–40% TFA, or temperature, 25–50° (Bradbury and Rattle, 1968). Specific solvent interactions contributions, alone, are rejected inasmuch as anisotropic shielding effects of this magnitude from a solvent molecule at the required CH–solvent distance is not possible (Stewart *et al.*, 1967a). As polymer–solvent interaction contributions to δ_{CH} must be rejected as the major contributor to the large nmr chemical shifts that are observed, we must conclude that changes in b_0 for this system do not reflect the degree of polymer helicity and that PLA continues to undergo dimensional changes throughout the range of acid concentration considered to support the helical configuration.

Bradbury and Rattle (1968) have interpreted b_0 and nmr results differently. Noting that in TFA-dichloroacetic acid and $CDCl_3$–dichloroacetic acid b_0 for PLA can be as much as twenty five percent lower than the value in TFA–$CHCl_3$, these investigators postulate that the helical content of the polymer is greater in the former solvent than the latter. As further substantiation of their positions, they interpret nmr line widths, greater in the former than the latter solvents, as due to restricted motion accompanying an increase in PLA helical content. We note comparable CH broadening line widths change from 20 Hz to approximately 30 Hz in appropriate regions near phase separations (Figure 11), but for both PLA and PDLA. We interpreted this line-width variation to be due to polypeptide–solvent and polypeptide–polypeptide interactions inasmuch as helical content changes are excluded for PDLA. We further note a modest decrease (about 8%) in b_0 for PLA in TFA–$CHCl_3$ near phase separation (Stewart *et al.*, 1967a), and ascribed this variation and that in the Bradbury and Rattle solvents, again, to intermolecular interactions.

Although phase separation is a rather common occurrence for random coil polymers in various solvent systems, this study as well as other preliminary studies indicate that helical polypeptides and other biopolymers generally undergo liquid–liquid-phase separation in appropriate mixtures of TFA–$CHCl_3$. In particular, PLA-phase separations in TFA–$CHCl_3$ mixtures at that point where the change in b_0 in the indicated solvent system (Stewart *et al.*, 1967a) appears to be still increasing, *i.e.*, the polymer has not completed interconversion to maximum helicity.

It has been recently reported (Ferretti, 1967; Bradbury *et al.*, 1968) that certain polypeptides can provide nmr spectral results indicating the amount of helix and random coil content of the polymer by direct observation of spectral features that can be ascribed to individual helical and random coil polymer portions. We note that the difference effects observed in their studies occur in precisely that region where phase separation may occur. In fact, if simultaneous nmr signals were obtained from the separated phases as indicated in the appropriately identified portion of Figure 6, for example, results similar to Ferretti and Bradbury *et al.*, could be obtained. As indicated above we have made preliminary studies of phase separation of the solutions examined by Ferretti and Bradbury *et al.*, and find that phase separation does occur and, in addition, is markedly affected by small quantities of water. Considerable care must, therefore, be exercised in concluding that individual spectral features exist in such solvent systems until detailed phase coexistence studies are made and the similar spectral features that arise from this phenomena can be discounted.

References

Abragam, A. (1961), The Principles of Nuclear Magnetism, London, Oxford University.

Bamford, C. H., Elliott, A., and Hanby, W. E. (1956), Synthetic Polypeptides, New York, N. Y., Academic.

Bradbury, E. M., Crane-Robinson, C., Goldman, H., and Rattle, H. W. E. (1968), *Nature 217*, 812.

Bradbury, E. M., Crane-Robinson, C., and Rattle, H. W. E. (1967), *Nature 216*, 862.

Bradbury, E. M., and Rattle, H. W. E. (1968), *Polymer 9*, 201.

Brown, L., and Trotter, I. F. (1956), *Trans. Faraday Soc. 52*, 537.

Doty, P., and Yang, J. T. (1956), *J. Am. Chem. Soc. 78*, 498.

Eizner, Y. E., and Ptitsyn, O. B. (1962), *Vysokomol. Soed. 4*, 1725.

Ferretti, J. A. (1967), *Chem. Commun.*, 1030.

Flory, P. J. (1953), Principles of Polymer Chemistry, Ithaca, N. Y., Cornell University.

Flory, P. J. (1956), *Proc. Roy. Soc. (London) A234*, 60.

Flory, P. J., and Fox, T. G (1951), *J. Am. Chem. Soc.* **73**, 1904.
Flory, P. J., and Leonard, Jr., W. J. (1965), *J. Am. Chem. Soc. 87*, 2102.
Flory, P. J., and Miller, W. G. (1966), *J. Mol. Biol. 15*, 298.
Glick, R. E., Stewart, W. E., and Mandelkern, L. (1966), *Biochim. Biophys. Acta 120*, 302.
Hanlon, S. (1966), *Biochemistry 5*, 2049.
Hanlon, S., and Klotz, I. M. (1965), *Biochemistry 4*, 37.
Mandelkern, L. (1964), Crystallization of Polymers, New York, N. Y., McGraw-Hill.
Markley, J. L., Meadows, D. H., and Jardetky, O. (1967), *J. Mol. Biol. 27*, 25.
Miller, W. G., Brant, D. A., and Flory, P. J. (1967), *J. Mol. Biol. 23*, 67.
Nagai, K. (1961), *J. Chem. Phys. 34*, 887.
Oya, M., Kuno, K., and Iwakura, Y. (1966), *Kogyo Kagaku Zashi 69*, 741.
Quadrifoglio, F., and Urry, D. W. (1967), *J. Phys. Chem. 71*, 2364.
Stake, M. A., and Klotz, I. M. (1966), *Biochemistry 5*, 1726.
Stewart, W. E., Mandelkern, L., and Glick, R. E. (1967a), *Biochemistry 6*, 143.
Stewart, W. E., Mandelkern, L., and Glick, R. E. (1967b), *Biochemistry 6*, 150.
Teramoto, A., Nakagawa, K., and Fujita, H. (1967), *J. Chem. Phys. 46*, 4197.
Yu, H., and Stockmayer, W. H. (1967), *J. Chem. Phys. 47*, 1369.

Variations in Leucine Transfer Ribonucleic Acid in Mouse Plasma Cell Tumors Producing κ-Type Immunoglobin Light Chains*

J. Frederic Mushinski and Michael Potter

ABSTRACT: A comparison was made of the chromatographic profiles of leucyl transfer ribonucleic acid from normal mouse liver and from several murine plasma cell tumors all of which secrete a unique example of the same antigenic class (κ) of immunoglobulin light chain. Using the Freon–Aliquat 336 reversed-phase column at least five leucyl transfer ribonucleic acid peaks are seen in profiles from liver and several tumors, with stable, reproducible differences among them in the relative proportion of each isoaccepting species. Certain other tumors producing the same class of light-chain protein appear to be very deficient in peaks 3 and/or 5 suggesting that these tumors do not have significant amounts of these components normally found in mammalian transfer ribonucleic acid. It is suggested that these quantitative and qualitative variations in leucyl transfer ribonucleic acid within a very closely related group of similarly differentiated tissues indicate that the different leucyl transfer ribonucleic acid genes are under independent control.

Multiplicity of tRNAs has been established in bacteria and higher organisms (Doctor *et al.*, 1961; Weiss and Kelmers, 1967; Caskey *et al.*, 1968; Yang and Novelli, 1968a). In only a few cases so far has a correspondence been shown between the several isoaccepting tRNAs and the multiple codons for an amino acid (Weisblum *et al.*, 1962; von Ehrenstein and Dais, 1963; Kano-Sueoka *et al.*, 1968; Caskey *et al.*, 1968). Compared with a system having only a single translational equivalent (codon and adaptor) for each amino acid the existence of several code words and multiple tRNAs for a single amino acid could permit additional versatility in protein synthesis. Evolution has not diminished this degeneracy and, instead, may have found some special values and uses for alternate codon–anticodon combinations specifying a single amino acid in regulating processes in more complex higher organisms such as mammals. Manipulation of this degenerate adaptor system may play a role in differentiation of complex genomes (Holland *et al.*, 1967) or in regulation of intracellular protein synthesis (Kano-Sueoka and Sueoka, 1966; von Ehrenstein, 1966). It has been speculated that a flexible, but regulated, translational system for immunoglobulin molecules could, with genetic economy, greatly increase the number and variability of immunoglobulins an organism could generate (Potter *et al.*, 1965; Campbell, 1967; Mach *et al.*, 1967).

Owing to the greater complexity in higher organisms, we would not consider the translational machinery of a whole organism as is usually done in yeast or bacteria, but we have the opportunity to look at individual tissues

* From the Laboratory of Biology, National Cancer Institute, Bethesda, Maryland 20014. *Received November 5, 1968.*